Environmental Research 269 (2025) 120934

Contents lists available at ScienceDirect

Environmental Research

journal homepage: www.elsevier.com/locate/envres

Exploring Nile Red staining as an analytical tool for surface-oxidized microplastics

Wakaba Idehara [a,1], Yuya Haga [a,b,*,1], Hirofumi Tsujino [a,b,c], Yudai Ikuno [b], Sota Manabe [a], Mii Hokaku [a], Haruyasu Asahara [a,b,d], Kazuma Higashisaka [a,b,e], Yasuo Tsutsumi [a,b,d,f,**]

[a] School of Pharmaceutical Sciences, Osaka University, 1-6 Yamadaoka, Suita, Osaka, 565-0871, Japan
[b] Graduate School of Pharmaceutical Sciences, Osaka University, 1-6 Yamadaoka, Suita, Osaka, 565-0871, Japan
[c] Museum Links, Osaka University, 1-13 Machikaneyama, Toyonaka, Osaka, 560-0043, Japan
[d] Institute for Open and Transdisciplinary Research Initiatives, Osaka University, 1-1 Yamadaoka, Suita, Osaka, 565-0871, Japan
[e] Institute for Advanced Co-Creation Studies, Osaka University, 1-6 Yamadaoka, Suita, Osaka, 565-0871, Japan
[f] Global Center for Medical Engineering and Informatics, Osaka University, 2-2 Yamadaoka, Suita, Osaka, 565-0871, Japan

ARTICLE INFO

Keywords:
Microplastic analysis
Surface oxidation
Fluorescence imaging
Environmental monitoring
Carbonyl index

ABSTRACT

Microplastics (MPs), defined as plastic particles smaller than 5 mm, have garnered considerable attention owing to their potential biological impact on human health. These particles exhibit a range of physicochemical properties, including size, shape, and surface oxidation. Nile Red is a prominent tool for detecting microplastics, enabling staining for dynamic analyses within biological systems. However, the efficacy of Nile Red staining for surface-oxidized MPs remains unclear. Therefore, we applied Nile Red dye to stain surface-oxidized polyethylene and polyvinyl chloride and observed that both materials were effectively stained, although the fluorescence intensity varied according to different hydrophobic dynamics. Imaging analysis revealed a correlation between the fluorescence intensity score and the degree of surface oxidation, as determined using the carbonyl index calculated from attenuated total reflection-Fourier transform infrared spectroscopy data. Collectively, these findings offer novel analytical approaches for investigating environmental MPs, enhancing our understanding of their behavior and impact.

1. Introduction

Microplastics (MPs), plastic particles with a diameter of less than 5 mm (Thompson et al., 2004; Arthur and Baker, 1959), are increasingly recognized as significant environmental pollutants posing potential risks to ecosystems and human health. Detection of MPs in various human samples, including blood (Leslie et al., 2022), lung (Jenner et al., 2022), placenta (Ragusa et al., 2021), feces (Yan et al., 2022), and atheroma tissue (Marfella et al., 2024), suggests widespread exposure. Therefore, comprehensive studies to understand their behaviors and effects are urgently needed.

The complex physicochemical properties of MPs, including size, shape, and surface modifications, present significant challenges for accurate analysis (Lim, 2021). A major hurdle is the absence of standard laboratory samples that effectively mimic the environmental counterparts of MPs (Rubin et al., 2021), especially in terms of diverse physicochemical properties. Additionally, the lack of labeled samples complicates efforts to investigate their kinetics effectively.

In response to these challenges, we developed a protocol for generating MPs that closely resemble those in the environment, focusing specifically on replicating surface chemical modifications (Ikuno et al., 2023, 2024). Since almost all the MPs are oxidized on their surface, we generated oxidized MPs by exposing them to vacuum ultraviolet rays. This protocol provides researchers with a valuable tool for conducting more accurate and representative studies on the behavior and effects of MPs.

Staining techniques, particularly using Nile Red, are crucial for enhancing the detection and analysis of MPs in the environment such as marine water or sewage sludge (Shruti et al., 2022). Nile Red is a lipophilic fluorescent dye with solvatochromic properties, meaning its

* Corresponding author. Graduate School of Pharmaceutical Sciences, Osaka University, 1-6, Yamadaoka, Suita, Osaka 565-0871, Japan.
** Corresponding author. School of Pharmaceutical Sciences, Osaka University, 1-6 Yamadaoka, Suita, Osaka, 565-0871, Japan.
E-mail addresses: haga-y@phs.osaka-u.ac.jp (Y. Haga), ytsutsumi@phs.osaka-u.ac.jp (Y. Tsutsumi).
[1] These two authors contributed equally to this work.

https://doi.org/10.1016/j.envres.2025.120934
Received 31 October 2024; Received in revised form 5 January 2025; Accepted 22 January 2025
Available online 23 January 2025

fluorescence emission spectrum shifts depending on the polarity of its environment (Gajo et al., 2024). In more polar surroundings, it displays a red-shift, resulting in longer wavelength emissions (Owen Tuck et al., 2009). This characteristic makes Nile Red particularly useful for detecting and distinguishing between different polymer types, as it can indicate variations in polarity associated with each polymer (Sturm et al., 2021). However, the application of Nile Red staining to environmentally mimicked MPs, especially those with surface oxidation and varying fluorescence ranges, remains largely unexplored. In particular, how surface oxidation changes the staining pattern has not been thoroughly examined, despite the fact that environmental MPs often undergo surface degradation.

Accordingly, in this study, we addressed these gaps by applying Nile Red staining to MPs generated using our protocol and focusing on surface modifications, as well as crucial physicochemical properties. We aimed to provide insights to assess the efficacy of this analytical tool via Nile Red staining in distinguishing between different types of MPs. Overall, our findings might contribute to the advancement of analytical techniques for studying environmental surface oxidazed MPs.

2. Materials and methods

2.1. Reagents

Nile Red was purchased from Sigma-Aldrich (St. Louis, MO, USA). Polyethylene (PE) particles (Flo-thene), with a medium particle size of 180 μm per the manufacturer's information, were purchased from Sumitomo Seika Chemicals Company (Osaka, Japan). Polyvinyl chloride (PVC) particles were obtained from Sigma-Aldrich, with a particle size of 80–120 μm determined via microscopic observation.

2.2. Sample preparation

We previously reported an oxidization method for PE and confirmed its successful oxidization (Ikuno et al., 2023). Briefly, to oxidize PE and PVC, we utilized a FLAT EXCIMER EX-mini (Hamamatsu Photonics K. K., Shizuoka, Japan) emitting UV light with a wavelength of 172 nm and dimensions of 86 × 40 mm. Initially, the sample was evenly spread on the bottom of a Petri dish, positioned approximately 10 mm from the light source, and exposed to UV light for 0.5, 1, and 2 h for PE or 5, 10, and 20 min for PVC. Subsequently, the treated PE and PVC samples were collected in sample bottles. PE and PVC without UV light exposure are presented as non-oxidized samples (0 h or 0 min for PE and PVC, respectively). Before and after degradation, particle size and shape are not changed through microscopic observation (data not shown), indicating that the UV treatment primarily affects the chemical structure rather than the physical morphology of the particles. We have previously confirmed that oxidized PE samples, prepared using a VUV wavelength of 172 nm, exhibit surface characteristics similar to those of environmental PE-MPs, as determined by XPS, SEM, and IR analysis (Ikuno et al., 2024).

2.3. ATR-IR measurement

To assess the oxidation of PE and PVC, attenuated total reflection infrared (ATR-IR) spectra were acquired using an Fourier Transform Infrared Spectroscopy (FTIR) Spectrum Two instrument (PerkinElmer, Waltham, MA, USA) equipped with a TGS detector. A diamond Attenuated Total Reflectance (ATR) crystal set at an incident angle of 45° to achieve approximately one reflection was utilized within a horizontal ATR accessory for sample measurement. Spectra were collected over the range of 4000–450 cm^{-1} with 8 scans at a resolution of 8 cm^{-1}.

Initially, a background spectrum devoid of any sample (air) was recorded on the ATR crystal, followed by the immediate measurement of the sample. The specimens were then placed on an ATR crystal and pressed to ensure proper contact. The IR spectra of the PE samples were subsequently obtained. The raw spectra were presented as the pATR (=−log I/I0) spectra, where the sample spectral intensity (I) was normalized by the background spectral intensity (I0) immediately preceding the sample measurement. Each value was normalized to the maximum value for each condition to normalize the IR spectra.

2.4. Carbonyl index

We used the carbonyl index to quantify the extent of oxidation, and we employed the carbonyl index (Almond et al., 2020). Carbonyl index is commonly utilized to assess the level of oxidation of MPs. This index was determined by evaluating the ratio of the peak height corresponding to the C=O bond (at 1714 cm^{-1}) to that of the CH_2 bond (at 1466 cm^{-1}) for PE, and similarly for PVC, by comparing the peak height of the C=O bond (at 1724 cm^{-1}) with that of the CH_2 bond (at 1426 cm^{-1}).

2.5. Nile red staining

We modified the published protocol for Nile Red staining (Maes et al., 2017). Briefly, prepared particles were stained with 10 μg/mL Nile Red in (50% Ethanol in MilliQ) for 24 h at 50 °C. After staining, the stained MPs were washed thrice with ethanol and allowed to dry for further analysis.

2.6. Imaging analysis

Nile Red is a lipophilic fluorescent dye with solvatochromic properties that exhibits a red shift in highly polar environments, resulting in a longer emission wavelength (Owen Tuck et al., 2009). Nile Red-stained particles were imaged using a CellVoyager CV8000 (CV8000; Yokogawa, Tokyo, Japan). Given their chemical structures, two sets of excitation and emission filters were selected for analysis of the PE, surface-oxidized PE, PVC and surface oxidized PVC. Particles were imaged with 488 nm excitation and 525/50 nm emission filters and 561 nm excitation and 600/37 nm emission filters for PE. Additionally, 561 nm excitation and 600/37 nm emission filters, as well as 640 nm excitation and 676/29 nm emission filters, were used for the PVC. Subsequently, the images were processed using Fiji (version: 2.9.0/1.53t, National Institutes of Health, Bethesda, MD, USA) and analyzed using CellProfiler 4.2.1 (Stirling et al., 2021) to quantify the fluorescence intensity of each particle. At least 40 particles (up to over 200 particles) from each condition were analyzed. The mean intensities of each particle were utilized to generate graphs using R software (R).

2.7. Statistical analyses

Graphs were generated using Prism 10 for MacOS (GraphPad Software, San Francisco, CA, USA) and the R software (R). Statistical analyses were performed using the R software (R). The data are presented as boxplots, with each value represented by a dotted line. P-values and R-values were calculated using Pearson correlation analysis with the stat_cor function in the ggplot2 library in R software (R). Statistical significance was set at $P < 0.05$.

3. Results and discussion

3.1. Generation of surface-oxidized PE and PVC

Surface-oxidized PE and PVC were generated in air using vacuum ultraviolet (VUV) light at a wavelength of 172 nm. The ATR-IR spectra of PE particles before and after VUV exposure are shown in Fig. 1A. A peak around 1466 cm^{-1} was due to CH_2 bending band. In addition, C=O stretching band (1714 cm^{-1}) appeared after VUV exposure. This spectra change demonstrated that carbonyl groups were introduced into PE in a time-dependent manner, indicating that PE samples were successfully oxidized by VUV exposure. The ATR-IR spectra of PVC particles before

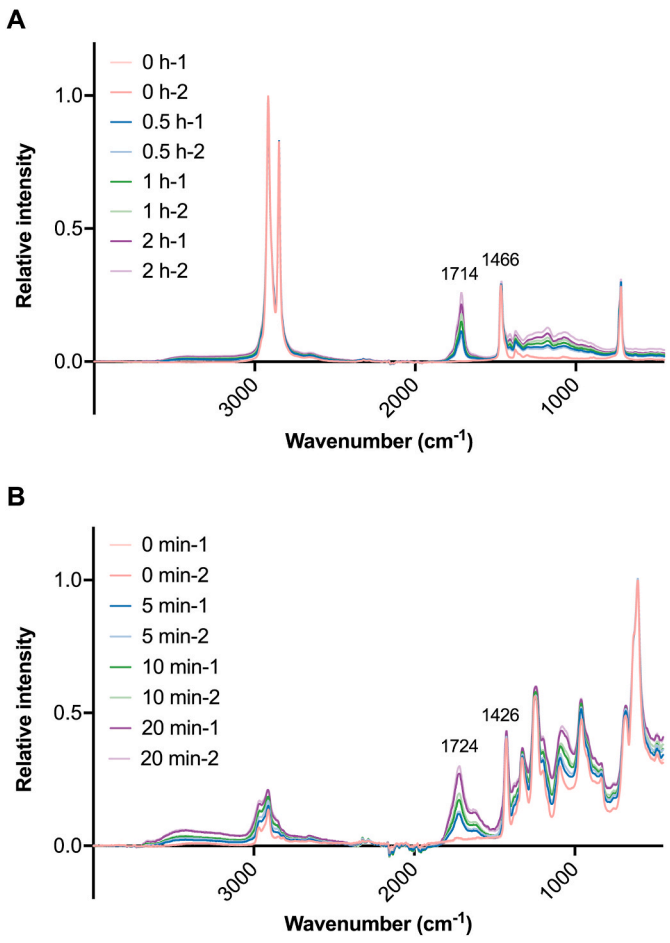

Fig. 1. ATR-IR spectra for oxidized PE and PVC. (A) Normalized attenuated total reflectance infrared spectra of PE samples at varying VUV exposure times (0, 0.5, 1, and 2 h). **(B)** Normalized attenuated total reflectance infrared spectra of PVC samples at varying VUV exposure times (0, 5, 10, and 20 min).

and after VUV exposure are shown in Fig. 1B. A peak around 1426 cm^{-1} was due to CH_2 bending band. In addition, C=O stretching band (1724 cm^{-1}) appeared after VUV exposure. Similary to PE, this change indicated that the time-dependent introduction of carbonyl groups were introduced into PVC particles.

3.2. Application of Nile red to surface-oxidized PE and PVC

As previously reported, the excitation and emission spectra of Nile Red-stained microplastics vary depending on the polymer type, specifically the hydrophobicity of the surface environment (Sancataldo et al., 2020). PE is more hydrophobic than PVC, which is why PVC exhibits fluorescence at longer wavelengths. Consequently, distinct wavelengths were selected for each polymer type. Additionally, Nile Red is a lipophilic fluorescent dye with solvatochromic properties that exhibits a red shift in highly polar environments, resulting in a longer emission wavelength (Owen Tuck et al., 2009). Upon VUV irradiation, the fluorescence intensity of PE altered; the fluorescent singals at 488 nm excitation with a 525/50 nm emission filter were detected in the non-oxidized sample but decreased with VUV oxidation, whereas the second fluorescent set, utilizing 561 nm excitation with a 600/37 nm emission filter, was almost undetectable in the non-oxidized sample but increased in a time-dependent manner (Fig. 2A). Considering the chemical structures of PVC, for the PVC samples, we employed 561 nm excitation with 600 nm emission filters and 640 nm excitation with 676/29 nm emission filters, showing dynamic changes in fluorescence intensity; upon VUV exposure, both fluorescence signals were increased (Fig. 2B).

3.3. Assessment of Nile red staining and extent of oxidation in PE and PVC materials

As depicted in Fig. 2, oxidized MPs demonstrated varied fluorescence intensities across channels in both PE and PVC samples. Thus, we analyzed the correlation between the carbonyl index and the fluorescence intensity ratio of each channel. The carbonyl index is a widely used measure for determining the oxidation level of MPs (Almond et al., 2020). It is calculated by comparing the peak height of the C=O bond (1714 cm−1) to that of the CH_2 bond (1466 cm−1) in PE (Fig. 1A). For PVC, the carbonyl index is similarly determined by comparing the peak height of the C=O bond (1724 cm−1) to that of the CH_2 bond (1426 cm−1) (Fig. 1B). In PE samples, particles were identified using CellProfiler software, and the fluorescence intensities of green (488 nm excitation and 525/50 nm emission) and yellow (561 nm excitation and 600/37 nm emission) were measured. Although the mean intensities of green and yellow fluorescence did not vary with VUV exposure time (Supplementary Figs. 1A and 1B), the ratio of yellow to green fluorescence (PE fluorescence score) increased in an exposure time-dependent manner (Fig. 3A). Furthermore, by using the median value to account for variability in the stained particles, a correlation existed between the carbonyl index of each sample and the median PE fluorescence score under each condition (Fig. 3B). Although increasing the number of analyzed particles and experimental trials to refine the correlation line would improve the robustness of these findings, the ratio of yellow to green fluorescence shows potential as an indicator of the oxidation rate in PE samples.

In PVC samples, Nile Red staining indicated a shift in emission wavelength to a longer wavelength with increasing polymer polarity (Sturm et al., 2021; Maes et al., 2017). Yellow and red fluorescence intensity increased with VUV exposure time (Supplementary Figs. 1C and 1D). To evaluate the correlation between the carbonyl index and the values derived from yellow and red fluorescence intensities, we assessed the mean fluorescence intensities of yellow and red in each particle (PVC fluorescence score). As shown in Fig. 3C, the PVC fluorescence score for each particle increased with VUV exposure time. Furthermore, by using the median PVC fluorescence score to account for variability, a correlation was observed between the carbonyl index and the median fluorescence score (Fig. 3D). Although increasing the number of analyzed particles and experimental trials to refine the correlation line would improve the robustness of these findings, the mean values of yellow and red fluorescence collectively serve as effective indicators for assessing oxidation in PVC samples.

Our investigation revealed distinct fluorescence patterns in different polymer types in response to oxidation. Nile Red fluorescence varies with polymer polarity (Sturm et al., 2021; Maes et al., 2017). As microplastics undergo changes in surface polarity owing to oxidative treatment (Kim et al., 2022), distinct fluorescence patterns emerge. Specifically, in PE samples, green fluorescence decreased upon oxidation, while yellow fluorescence increased. Conversely, in PVC samples, both yellow and red fluorescence increased. For PE, calculating the ratio of green-to-yellow fluorescence revealed a correlation with the degree of oxidation, whereas, for PVC, the average yellow and red fluorescence correlated with the degree of oxidation. These findings highlight the utility of Nile Red as a tool for analyzing the oxidation of PE and PVC MPs, suggesting its applicability in analysis of environmental oxidized MPs.

Since Nile Red is a solvatochromic reagent, stained particles emit different fluorescence intensities depending on their hydrophobic or hydrophilic nature (Owen Tuck et al., 2009; Meyers et al., 2022). As reported in previous studies (Sturm et al., 2021; Kang et al., 2020; Van et al., 2020), Nile Red staining can be applied to a wide range of polymers, including PE, polypropylene (PP), polystyrene (PS), polyethylene

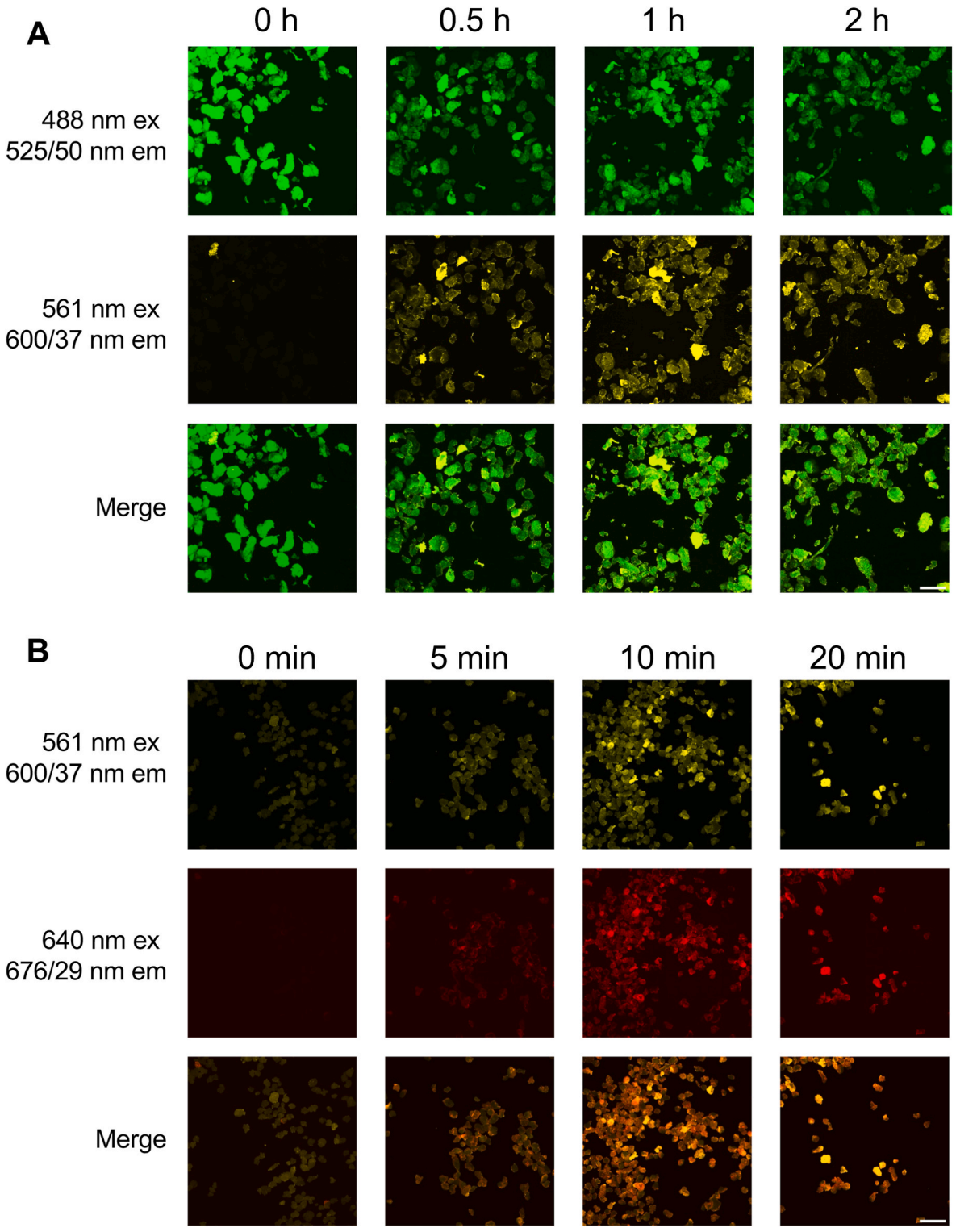

Fig. 2. Fluorescence images of Nile Red-stained PE and PVC particles. (A) Fluorescence images of PE samples at different VUV exposure times (0, 0.5, 1, and 2 h). **(B)** Fluorescence images of PVC samples at varying VUV exposure times (0, 5, 10, and 20 min). Representative images from two experiments are displayed. Scale bar: 500 μm.

terephthalate (PET), polyester, PVC, and polyamide (PA), regardless of their polarity or hydrophobicity. While further investigation is needed to determine the extent of fluorescence shifts and polarity changes due to oxidative degradation, as well as to ensure proper calibration for each polymer type to improve the accuracy of our analysis, this method shows potential for application to various polymer types beyond PE and PVC.

As Nile Red is typically used to stain lipids in cellular components (Greenspan et al., 1985), applying our method for MP analysis in tissues requires the removal of tissue components and the isolation of plastic debris. Previous studies have demonstrated effective methods for tissue digestion and component removal (Di Fiore et al., 2024), enabling the application of our method for MP detection in tissue samples.

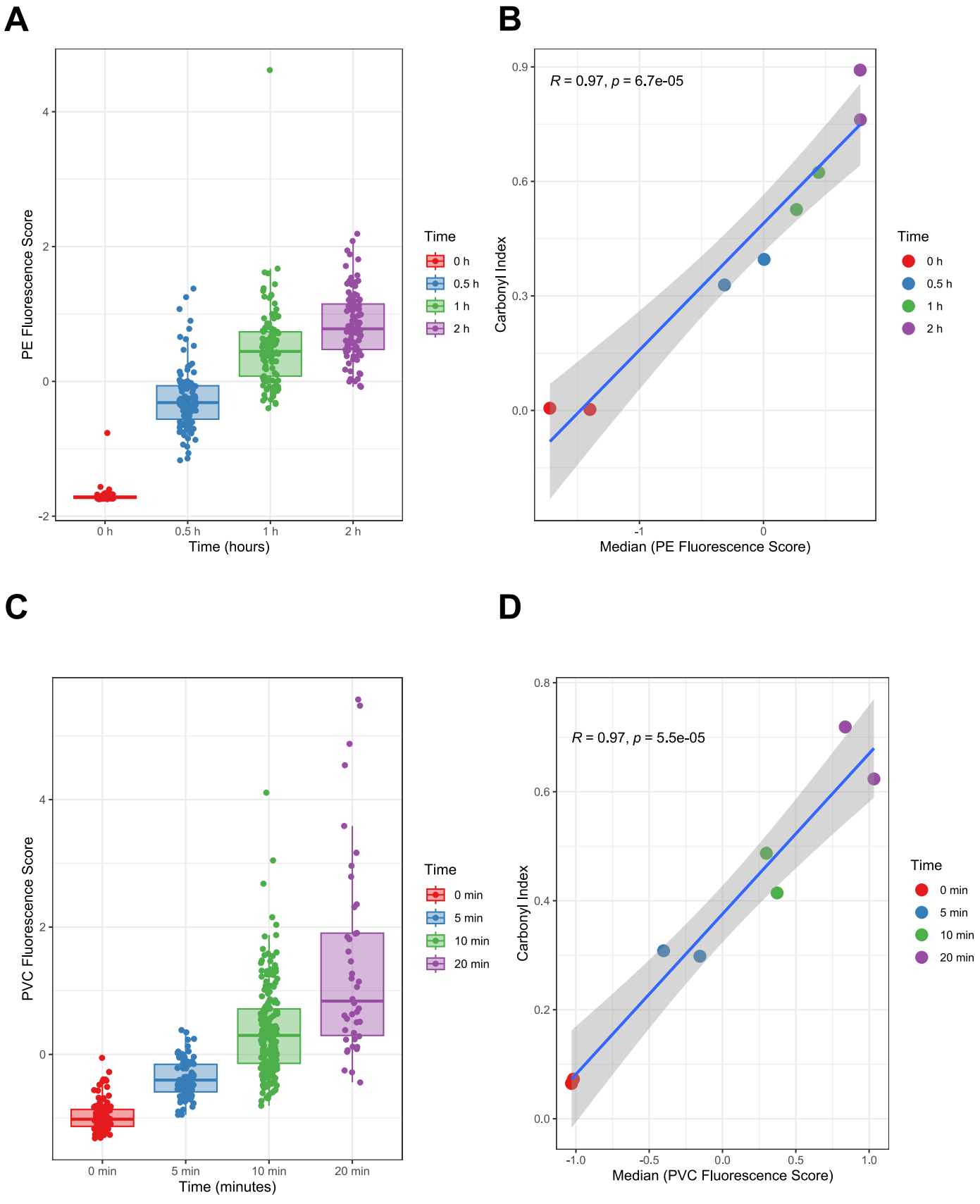

(caption on next page)

Fig. 3. Correlation analysis of fluorescence intensity and carbonyl index. (A) Boxplots illustrating the PE fluorescence score, the scaled ratio of yellow fluorescence (561 nm excitation and 600/37 nm emission filter) to green fluorescence (488 nm excitation and 525/50 nm emission filter) at various VUV exposure times (0, 0.5, 1, and 2 hours), with each value represented as dots. Representative data from two experiments are presented. **(B)** Correlation plot of carbonyl index and median value of PE fluorescence score at each VUV exposure time. The plot includes data points after 0, 0.5, 1, and 2 hours of VUV exposure, from two independent experiments, totaling eight points. The carbonyl index for each point was calculated using spectra data from Fig. 1A.**(C)** Boxplots displaying the PVC fluorescence score, the scaled mean of yellow fluorescence (561 nm excitation and 600/37 nm emission filter), and red fluorescence (640 nm excitation and 676/29 nm emission filter) at varying VUV times (0, 5, 10, and 20 minutes), with each value represented as dots. Representative data from two experiments are presented. **(D)** Correlation plot of carbonyl index and median value of PE fluorescence score at each VUV exposure time. The plot includes data points after 0, 5, 10, and 20 minutes of VUV exposure, from two independent experiments, totaling eight points. The carbonyl index for each point was calculated using spectra data from Fig. 1B.

In the case of environmental samples comprising a mixture of different materials, a statistical approach utilizing histograms would likely be the most suitable method for analysis. Additionally, by isolating individual particles from environmental samples and examining the correlation between the Nile Red method and IR measurements, a more robust analytical approach for environmental MPs could be developed. Regarding the oxidation method, a VUV wavelength of 172 nm was used in this study. However, considering natural environmental conditions, future analyses may benefit from utilizing wavelengths around 300 nm, such as those produced by xenon lamp irradiation.

4. Conclusions

VUV exposure successfully generated oxidized PE and PVC MPs, resulting in altered fluorescence signals from Nile Red staining. The correlation observed between fluorescence scores and the carbonyl index of oxidized MPs underscores the potential of Nile Red as an effective tool for analyzing the oxidation state of PE and PVC MPs, supporting its use in environmental studies of oxidized MPs.

CRediT authorship contribution statement

Wakaba Idehara: Writing – review & editing, Visualization, Validation, Investigation, Formal analysis. **Yuya Haga:** Writing – original draft, Visualization, Project administration, Investigation, Formal analysis, Conceptualization. **Hirofumi Tsujino:** Writing – review & editing, Conceptualization. **Yudai Ikuno:** Writing – review & editing, Investigation, Formal analysis. **Sota Manabe:** Investigation, Formal analysis. **Mii Hokaku:** Investigation, Formal analysis. **Haruyasu Asahara:** Writing – review & editing. **Kazuma Higashisaka:** Writing – review & editing. **Yasuo Tsutsumi:** Writing – review & editing, Supervision, Project administration, Funding acquisition, Conceptualization.

Funding sources

This work was supported by the Environment Research and Technology Development Fund (JPMEERF20241003) of the Environmental Restoration and Conservation Agency provided by Ministry of the Environment of Japan, Japan Society for the Promotion of Science (Grant Number 21K19336), Japan Ministry of Health, Labor and Welfare (Grant Number JPMH21447937), and The Sumitomo Foundation for Environmental Research Projects.

Declaration of competing interest

The authors declare that they have no known competing financial interests or personal relationships that could have appeared to influence the work reported in this paper.

Acknowledgment

The authors express their gratitude to Dr. Kei Ohkubo and Dr. Yuki Itabashi of the Institute for Open and Transdisciplinary Research Initiatives, Osaka University, Osaka, Japan, for providing us with the opportunity to use the FLAT EXCIMER EX-mini. This research was partially supported by the Research Support Project for Life Science and Drug Discovery (Basis for Supporting Innovative Drug Discovery and Life Science Research) from AMED under Grant Number JP24ama121054.

Appendix A. Supplementary data

Supplementary data to this article can be found online at https://doi.org/10.1016/j.envres.2025.120934.

Data availability

Data will be made available on request.

References

Almond, J., Sugumaar, P., Wenzel, M.N., Hill, G., Wallis, C., 2020. Determination of the carbonyl index of polyethylene and polypropylene using specified area under band methodology with ATR-FTIR spectroscopy. E-Polym 20 (1), 369–381. https://doi.org/10.1515/epoly-2020-0041.

Arthur, Courtney, Baker, Joel E., 1959. Bamford, holly A.; corporate authors(s) : United States, national ocean service., office of response and restoration; conference author (s) : international research workshop on the occurrence, effects, and fate of microplastic marine debris 2008 : tacoma, wash.), sponsor. Proceedings of the International Research Workshop on the Occurrence, Effects, and Fate of Microplastic Marine Debris, September 9-11, 2008, University of Washington Tacoma, Tacoma, WA, USA, 2009. https://repository.library.noaa.gov/view/noaa/2509.

Di Fiore, C., Ishikawa, Y., Wright, S.L., 2024. A review on methods for extracting and quantifying microplastic in biological tissues. J. Hazard Mater. 464, 132991. https://doi.org/10.1016/j.jhazmat.2023.132991.

Gajo, C., Shchepanovska, D., Jones, J.F., Karras, G., Malakar, P., Greetham, G.M., Hawkins, O.A., Jordan, C.J.C., Curchod, B.F.E., Oliver, T.A.A., 2024. Nile red fluorescence: where's the twist? J. Phys. Chem. B 128 (47), 11768–11775. https://doi.org/10.1021/acs.jpcb.4c06048.

Greenspan, P., Mayer, E.P., Fowler, S.D., 1985. Nile red: a selective fluorescent stain for intracellular lipid droplets. J. Cell Biol. 100 (3), 965–973. https://doi.org/10.1083/jcb.100.3.965.

Ikuno, Y., Tsujino, H., Haga, Y., Asahara, H., Higashisaka, K., Tsutsumi, Y., 2023. Impact of degradation of polyethylene particles on their cytotoxicity. Microplastics 2 (2), 192–201. https://doi.org/10.3390/microplastics2020015.

Ikuno, Y., Tsujino, H., Haga, Y., Manabe, S., Idehara, W., Hokaku, M., Asahara, H., Higashisaka, K., Tsutsumi, Y., 2024. Polyethylene, whose surface has been modified by UV irradiation, induces cytotoxicity: a comparison with microplastics found in beaches. Ecotoxicol. Environ. Saf. 277, 116346. https://doi.org/10.1016/j.ecoenv.2024.116346.

Jenner, L.C., Rotchell, J.M., Bennett, R.T., Cowen, M., Tentzeris, V., Sadofsky, L.R., 2022. Detection of microplastics in human lung tissue using μFTIR spectroscopy. Sci. Total Environ. 831, 154907. https://doi.org/10.1016/j.scitotenv.2022.154907.

Kang, H., Park, S., Lee, B., Ahn, J., Kim, S., 2020. Modification of a nile red staining method for microplastics analysis: a nile red plate method. Water 12 (11), 3251. https://doi.org/10.3390/w12113251.

Kim, S., Sin, A., Nam, H., Park, Y., Lee, H., Han, C., 2022. Advanced oxidation processes for microplastics degradation: a recent trend. Chem. Eng. J. Adv. 9, 100213. https://doi.org/10.1016/j.ceja.2021.100213.

Leslie, H.A., Van Velzen, M.J.M., Brandsma, S.H., Vethaak, A.D., Garcia-Vallejo, J.J., Lamoree, M.H., 2022. Discovery and quantification of plastic particle pollution in human blood. Environ. Int. 163, 107199. https://doi.org/10.1016/j.envint.2022.107199.

Lim, X., 2021. Microplastics are everywhere — but are they harmful? Nature 593 (7857), 22–25. https://doi.org/10.1038/d41586-021-01143-3.

Maes, T., Jessop, R., Wellner, N., Haupt, K., Mayes, A.G., 2017. A rapid-screening approach to detect and quantify microplastics based on fluorescent tagging with nile red. Sci. Rep. 7 (1), 44501. https://doi.org/10.1038/srep44501.

Marfella, R., Prattichizzo, F., Sardu, C., Fulgenzi, G., Graciotti, L., Spadoni, T., D'Onofrio, N., Scisciola, L., La Grotta, R., Frigé, C., Pellegrini, V., Municinò, M., Siniscalchi, M., Spinetti, F., Vigliotti, G., Vecchione, C., Carrizzo, A., Accarino, G., Squillante, A., Spaziano, G., Mirra, D., Esposito, R., Altieri, S., Falco, G., Fenti, A., Galoppo, S., Canzano, S., Sasso, F.C., Matacchione, G., Olivieri, F., Ferraraccio, F., Panarese, I., Paolisso, P., Barbato, E., Lubritto, C., Balestrieri, M.L., Mauro, C.,

Caballero, A.E., Rajagopalan, S., Ceriello, A., D'Agostino, B., Iovino, P., Paolisso, G., 2024. Microplastics and nanoplastics in atheromas and cardiovascular events. N. Engl. J. Med. 390 (10), 900–910. https://doi.org/10.1056/NEJMoa2309822.

Meyers, N., Catarino, A.I., Declercq, A.M., Brenan, A., Devriese, L., Vandegehuchte, M., De Witte, B., Janssen, C., Everaert, G., 2022. Microplastic detection and identification by nile red staining: towards a semi-automated, cost- and time-effective technique. Sci. Total Environ. 823, 153441. https://doi.org/10.1016/j.scitotenv.2022.153441.

Owen Tuck, P., Christopher Mawhinney, R., Rappon, M., 2009. An ab initio and TD-DFT study of solvent effect contributions to the electronic spectrum of nile red. Phys. Chem. Chem. Phys. 11 (22), 4471. https://doi.org/10.1039/b902528f.

The R Project for statistical computinghttps://www.r-project.org/.

Ragusa, A., Svelato, A., Santacroce, C., Catalano, P., Notarstefano, V., Carnevali, O., Papa, F., Rongioletti, M.C.A., Baiocco, F., Draghi, S., D'Amore, E., Rinaldo, D., Matta, M., Giorgini, E., 2021. Plasticenta: first evidence of microplastics in human placenta. Environ. Int. 146, 106274. https://doi.org/10.1016/j.envint.2020.106274.

Rubin, A.E., Sarkar, A.K., Zucker, I., 2021. Questioning the suitability of available microplastics models for risk assessment – a critical review. Sci. Total Environ. 788, 147670. https://doi.org/10.1016/j.scitotenv.2021.147670.

Sancataldo, G., Avellone, G., Vetri, V., 2020. Nile red lifetime reveals microplastic identity. Environ. Sci. Process. Impacts 22 (11), 2266–2275. https://doi.org/10.1039/D0EM00348D.

Shruti, V.C., Pérez-Guevara, F., Roy, P.D., Kutralam-Muniasamy, G., 2022. Analyzing microplastics with nile red: emerging trends, challenges, and prospects. J. Hazard Mater. 423, 127171. https://doi.org/10.1016/j.jhazmat.2021.127171.

Stirling, D.R., Swain-Bowden, M.J., Lucas, A.M., Carpenter, A.E., Cimini, B.A., Goodman, A., 2021. CellProfiler 4: improvements in speed, utility and usability. BMC Bioinf. 22 (1), 433. https://doi.org/10.1186/s12859-021-04344-9.

Sturm, M.T., Horn, H., Schuhen, K., 2021. The potential of fluorescent dyes—comparative study of nile red and three derivatives for the detection of microplastics. Anal. Bioanal. Chem. 413 (4), 1059–1071. https://doi.org/10.1007/s00216-020-03066-w.

Thompson, R.C., Olsen, Y., Mitchell, R.P., Davis, A., Rowland, S.J., John, A.W.G., McGonigle, D., Russell, A.E., 2004. Lost at sea: where is all the plastic? Science 304 (5672). https://doi.org/10.1126/science.1094559, 838–838.

Van Raamsdonk, L.W.D., Van Der Zande, M., Koelmans, A.A., Hoogenboom, R.L.A.P., Peters, R.J.B., Groot, M.J., Peijnenburg, A.A.C.M., Weesepoel, Y.J.A., 2020. Current insights into monitoring, bioaccumulation, and potential Health effects of microplastics present in the food chain. Foods 9 (1), 72. https://doi.org/10.3390/foods9010072.

Yan, Z., Liu, Y., Zhang, T., Zhang, F., Ren, H., Zhang, Y., 2022. Analysis of microplastics in human feces reveals a correlation between fecal microplastics and inflammatory bowel disease status. Environ. Sci. Technol. 56 (1), 414–421. https://doi.org/10.1021/acs.est.1c03924.